


PAPER

[View Article Online](#)
[View Journal](#) | [View Issue](#)Cite this: *J. Mater. Chem. A*, 2021, 9, 26976

A dual-role electrolyte additive for simultaneous polysulfide shuttle inhibition and redox mediation in sulfur batteries†

Ayda Rafie, Rahul Pai and Vibha Kalra *

In Li–S batteries, the insulating nature of sulfur and Li₂S causes enormous challenges, such as high polarization and low active material utilization. The nucleation of the solid discharge product, Li₂S, during the discharge cycle, and the activation of Li₂S in the subsequent charge cycle, cause a potential challenge that needs to be overcome. Moreover, the shuttling of soluble lithium polysulfide intermediate species results in active material loss and early capacity fade. In this study, we have used thiourea as an electrolyte additive and showed that it serves as both a redox mediator to overcome the Li₂S activation energy barrier and a shuttle inhibitor to mitigate the notorious polysulfide shuttling via the investigation of thiourea redox activity, shuttle current measurements and study of Li₂S activation. The steady-state shuttle current of the Li–S battery shows a 6-fold drop when 0.02 M thiourea is added to the standard electrolyte. Moreover, by adding thiourea, the charge plateau for the first cycle of the Li₂S based cathodes shifts from 3.5 V (standard ether electrolyte) to 2.5 V (with 0.2 M thiourea). Using this additive, the capacity of the Li–S battery stabilizes at ~839 mA h g^{−1} after 5 cycles and remains stable over 700 cycles with a low capacity decay rate of 0.025% per cycle, a tremendous improvement compared to the reference battery that retains only ~350 mA h g^{−1} after 300 cycles. In the end, to demonstrate the practical and broad applicability of thiourea in overcoming sulfur-battery challenges and in eliminating the need for complex electrode design, we study two additional battery systems – lithium metal-free cells with a graphite anode and Li₂S cathode, and Li–S cells with simple slurry-based cathodes fabricated via blending commercial carbon black/S and a binder. We believe that this study manifests the advantages of redox active electrolyte additives to overcome several bottlenecks in the Li–S battery field.

Received 23rd April 2021
Accepted 13th October 2021

DOI: 10.1039/d1ta03425a

rsc.li/materials-a

1. Introduction

Lithium–sulfur (Li–S) batteries are considered to be one of the most promising next generation batteries owing to their high theoretical gravimetric energy density of ~2510 W h kg^{−1}, and highly abundant, cheap and non-toxic sulfur active material.¹ Nonetheless, there are challenges toward the commercialization of these batteries. The challenges on the cathode side are related to the insulating nature of sulfur (S₈) and Li₂S, volume expansion (~80%) in each discharge cycle, and most importantly, the shuttling of intermediate polysulfides causing rapid capacity fade.^{1–3} This past decade has seen extensive research with exemplary studies mitigating these challenges. The majority of this research has been focused on cathode design involving (1) complex cathode architectures,^{4,5} (2) novel cathode host chemistries,^{6–8} and/or (3) modification of sulfur active material through the formation of S–X covalent bonds (where X

can be carbon, metal, selenium, or phosphorus)^{9,10} to enhance the conductivity, accommodate volume expansion and physically and/or chemically entrap polysulfides.

However, an alternate and more economical solution is the engineering and design of electrolyte additives. While often overshadowed by the overwhelming literature on cathode modifications, electrolyte additives can play a vital role in enhancing the performance of Li–S batteries.^{11–13} They are usually added in very small fractions into the electrolyte and therefore, unlike cathode hosts, electrolyte additives would not typically hinder the achievable energy density of batteries.¹² Moreover, efficient electrolyte additives can potentially eliminate the need for a complicated cathode design.^{14,15} For these reasons, the Li-ion industry heavily relies on electrolyte additives as the most economical and efficient way to circumvent the issues and improve the battery performance.

Nevertheless, research on electrolyte additives for Li–S batteries has been limited. In the Li–S field, electrolyte additives with three primary roles have been investigated, all targeted toward polysulfide shuttling – (a) formation of a stable solid-electrolyte interphase (SEI) on the lithium anode¹⁶ to protect it from the shuttling polysulfides, (b) development of a stable

Department of Chemical and Biological Engineering, Drexel University, Philadelphia, PA, 19104, USA. E-mail: vk99@drexel.edu

† Electronic supplementary information (ESI) available. See DOI: 10.1039/d1ta03425a

cathode electrolyte interphase (CEI) to serve as a barrier to polysulfide diffusion at the cathode,¹² and (c) formation of complexes with intermediate polysulfides to decrease polysulfide shuttling.¹⁷ The most commonly used additive in Li-S batteries, LiNO_3 , is believed to reduce the adverse effects of polysulfide shuttling by the formation of a protective SEI layer on the Li metal anode.¹⁶ Such SEI formation on the lithium anode has also been explored using other additives such as LiI and P_2S_5 .¹⁸ In addition, additives such as fluorinated ethers or pyrrole can form a stable CEI on the sulfur cathode and act as a barrier layer to suppress/delay the diffusion of soluble polysulfides.¹² Another interesting example of additives used to improve the cycling stability of Li-S batteries is thiol-based additives, such as biphenyl-4,4'-dithiol (BPD).^{13,17} Being a redox active additive in the Li-S battery voltage range (1.8–2.6 V vs. Li/Li^+), this additive forms BPD-polysulfide complexes during the discharge step. The formation of such complexes results in changes in the reduction pathways and mechanisms of sulfur cathodes. Nevertheless, each of the additives studied plays a single role limited to the mitigation of polysulfide shuttling.

Overall, with limited literature on Li-S battery electrolyte additives, there is a need to expand the spectrum of additives that can play additional roles in mitigating Li-S chemistry challenges to truly eliminate the need for complex/expensive cathode design. To this end, in this work, we demonstrate thiourea as an additive that plays a “dual” role as both a polysulfide shuttle inhibitor and a redox mediator (RM). A redox mediator, if successful, can dramatically increase the electron transfer between the conductive host and active material without the need for physical contact, resulting in enhanced active material utilization.^{19,20} While RM-type additives have been widely used in Li-air batteries for Li_2O_2 utilization in each cycle,²¹ only a handful of reports investigated this concept in Li-S batteries.^{15,22} Moreover, to the best of our knowledge there is no study in the literature, where an additive is used simultaneously both as a redox mediator and as a polysulfide shuttle inhibitor. Thiourea (TU) has been previously used as an electrolyte additive to Li-air batteries, and SEI formation with and without this additive is investigated. In this work by Ho *et al.*, the effect of TU on suppressing the growth of Li dendrites is attributed to reduction in electrolyte decomposition in the presence of the TU additive.²³

In this work, we investigate thiourea as an organic electrolyte additive in Li-S batteries. The major part of the study is focused on lithium-sulfur cells composed of a lithium anode and free-standing carbon nanofiber-based (CNF) sulfur cathode. On addition of thiourea into the standard ether electrolyte, the cycle stability was increased by more than two-fold. Free-standing binder-free and current collector-free CNF was used as a cathode sulfur host to prevent interference from binders and/or current collectors in revealing the fundamental mechanism of TU activity in sulfur batteries. Through an investigation of TU redox activity, shuttle current measurements, and study of Li_2S activation, we show that thiourea serves as both a PS shuttle suppressing- and a redox mediating-additive. We discuss in the paper that TU facilitates shuttle suppression through the

formation of complexes between C-S^{\cdot} and polysulfide anion radicals. To demonstrate the role of TU as a redox mediator, we synthesized a Li_2S cathode (instead of sulfur) and showed that thiourea reduced the activation potential of Li_2S , an ionically and electronically insulating material, from 3.4 V to 2.54 V.

In the final part of this work, we study two additional battery/material systems to demonstrate the broad and practical applicability of the thiourea additive enabling cheaper and simpler electrodes – in the first example, TU enables a stable lithium metal-free battery composed of a commercial graphite anode and Li_2S nanofiber cathode with a stable capacity of 900 mA h g^{-1} for 400 cycles. In the second example, we show both coin cell and prototype pouch cell data, where TU enabled stable capacity for hundreds of charge-discharge cycles with simple industry-friendly sulfur slurry cathodes (made by just blending commercial sulfur with carbon black and PVDF binder), which are otherwise known to exhibit rapid capacity fade.

To the best of our knowledge, this work is the first ever study on the use of an electrolyte additive that enhances the performance of Li-S batteries as both a shuttle inhibitor and a redox mediator. These results are a significant initial step toward further studies on engineering electrolyte additives with multiple roles.

2. Experimental methods

2.1 Fabrication of SCNF/S and Li_2S /CNF cathodes

We used the electrospinning technique to fabricate carbon nanofibers (CNFs). The polymeric solution for electrospinning was prepared by dissolving polyacrylonitrile (PAN, average MW: 150 000 Sigma Aldrich) and dried LIQION (Nafion, Liquion 1105, Ion Power Inc.) in a ratio of 40 : 60 wt% in *N,N*-dimethylformamide (DMF, Sigma Aldrich).²⁴ A total solid concentration of 18% was used to prepare the solution. This solution was then loaded into syringes and electrospun using a 22-gauge needle (stainless steel needle, Hamilton Co.). The electrospinning was carried out using the following conditions: the flowrate was set to 0.2 mL h^{-1} , the distance between the needle and Al foil collector was between 15 and 16 cm, and the voltage was set between 9 and 10 kV to ensure smooth electrospinning. Electrospinning was carried out at room temperature, and the humidity in the electrospinning chamber was kept below 20% using zeolite desiccants. The electrospun nanofiber mats were then stabilized at 280°C for 6 h under air in a convection oven (Binder Inc, Germany). The stabilized samples were then carbonized in a tube furnace (MTI Co., USA) at 1000°C for 1 h under a continuous N_2 flow. The heating rate of the furnace was adjusted to 3°C min^{-1} both for heating and cooling steps. To incorporate sulfur, we used the “ultra-rapid melt diffusion” technique, developed in our lab.²⁵ In this technique, a desired amount of sulfur is sprinkled on CNFs, and a hot press is used to incorporate sulfur into the CNF matrix at 155°C for only 55 s using a slight pressure of $<250 \text{ psi}$. The Li_2S /CNF cathodes were synthesized by electrospinning a mixture of 0.5 g Li_2SO_4 (Sigma Aldrich) and 1 g polyvinylpyrrolidone (MW: 300 000, Sigma Aldrich) in a mixture of 4.5 g DI water, 3 g ethanol, and 1.5 g

acetone solvents. The electrospun fiber mats were then stabilized at 170 °C for 20 h under air and carbonized at 900 °C for 1 h under a continuous flow of Ar. The nanofibers were immediately transferred to a glovebox antechamber after the heat treatment to avoid any exposure to air.

2.2 Characterization of cathodes

Thermogravimetric analysis (TGA) on sulfur powder and SCNF cathodes was carried out on a TA 2950 (TA Instruments, USA), under a steady flow of N₂. A very low heating rate of 2.5 °C min⁻¹ was used to increase the temperature from room temperature to 800 °C. To measure the Li₂S content of Li₂S/CNF samples, anhydrous methanol was used to wash away the Li₂S particles and the weight of the sample was measured before and after the washing procedure. The measurements were carried out on three samples from three different batches, and the wt% of Li₂S particles was calculated to be 46.2 wt%. The formation of Li₂S is confirmed using X-ray diffraction (XRD), performed using a Rigaku MiniFlex 600. The Li₂S samples were sealed inside a glovebox using Kapton tape to avoid air exposure while transferring to the XRD instrument. The morphology of CNFs, Li₂S/CNFs, and SCNFs is investigated using a Zeiss Supra 50VP field-emission scanning electron microscope (SEM). The SEM instrument was equipped with an Oxford UltiMax 40 mm energy dispersive spectrometer (EDS), used for elemental mapping. A very thin layer of platinum was sputtered using a Cressington sputter coater to increase the conductivity of samples. The Li₂S samples were transferred using an air-tight container, sealed inside a glovebox; however, the samples were exposed to air for a very short period of time (~30 s) before transferring them to the SEM chamber. To collect the infrared spectra of the electrolyte with TU additive before and after exposure to Li metal, we used a Fourier transform infrared (FTIR) spectrometer (Nicolet iS50, Thermo Fisher Scientific), equipped with an extended range diamond ATR accessory and with a deuterated triglycine sulfate (DTGS) detector. The FTIR puck was transferred to a glovebox and 60 µL of the sample was used for each measurement. The puck was then sealed inside the glovebox avoid moisture and oxygen contamination. The spectra were collected with a resolution of 64 scans per spectrum at 8 cm⁻¹, and they were corrected using background and baseline correction and advanced ATR correction in the Thermo Scientific Omnic software package.

2.3 Coin cell and pouch cell fabrication and electrochemical testing

The Li₂S/CNF cathode was used without any further modification. The CNF cathodes (without any sulfur active material) were dried at 140 °C overnight using a convection oven. The CNF/SCNF electrodes were dried under vacuum before transferring them into a glovebox. The Li₂S/CNF, CNFs, and SCNFs were used without the need for any binder or current collector. For slurry cathodes, sulfur, PVDF binder, and Super P conductive carbon were used in a weight ratio of 50 : 10 : 40. An appropriate amount of NMP solvent was used and the solution was stirred overnight using a stirring plate. The slurry was then coated on

Al foil with different thicknesses using a doctor blade. The thickness of coating was adjusted to achieve a loading of 1.6 to 5 mg cm⁻² of sulfur. The slurry cathodes were then dried overnight under air and at 55 °C, and for 12 h under vacuum. The area of both freestanding and slurry cathodes was 0.855 cm². To fabricate the coin cells, we used CR2032 coin cells, stainless steel spacers and springs (all from MTI corporation), Li foil (Aldrich, punched to 13 mm diameter discs) as the anode, Li₂S/CNFs, SCNFs, CNFs and sulfur slurries as the cathode and a polypropylene separator (Celgard 2500; 19 mm diameter). To synthesize the ether-based electrolyte, we mixed 1.85 M LiCF₃SO₃ (99.995% trace metals basis, Sigma Aldrich) as salt and 0.1 M LiNO₃ (Acros Organics) (as an additive). The salt and additive used in this study were transferred to a glove box upon receiving without any further modification. We used a solution of 1,2-dimethoxyethane (DME, Acros Organics) and 1,3-dioxolane (DOL, Sigma Aldrich) at a 1 : 1 volume ratio as the solvent. To synthesize an ether-based electrolyte with the TU additive, we added an appropriate amount of thiourea (Sigma Aldrich) to achieve concentrations of 0.02 M, 0.2 M and 0.5 M in the electrolyte. The amount of electrolyte used in coin cells was set to 30 µL for all the SCNF and slurry-based cathodes except for the high loading cells (between 4 and 5 mg cm⁻²). The amount of electrolyte used for these cells was 80 µL. All the coin cells were rested for 4 hours at their open circuit voltage and conditioned at C/10 and C/5 (two cycles at each rate) before long-term cycling at C/2 between 1.8 and 2.7 V (vs. Li/Li⁺). For cells cycled at C/5, we conditioned the cells at C/20 and C/10 (for two cycles). Likewise, for cells cycled at C/10 we conditioned the cells at C/20 for two cycles. For the Li-S pouch cell, we have used the slurry-based cathode (25 cm²) with a Li metal foil anode rolled on copper foil. We used the ether electrolyte with the 0.2 M TU additive and sealed the pouch cell package under vacuum. In all the electrochemical testing where sulfur is used as the active material, 1C is 1675 mA h g⁻¹ and all the reported discharge capacities in the manuscript are based on the sulfur weight. Li metal-free coin cells were fabricated using Li₂S/CNFs as the cathode and graphite (single layer graphite coated on copper foil, MTI Corporation) as the anode. The graphite electrodes were used after drying overnight in a vacuum, without any further modification. In all these coin cells, 1C is considered as the theoretical capacity of Li₂S (~1166 mA h g⁻¹) and the discharge capacity reported is based on the weight of Li₂S in the cathode. For the coin cells fabricated using Li₂S/CNFs as the cathode material, the cells were first charged to 3.8 V for the first cycle at C/20, followed by conditioning cycles at C/10 and C/5 and long-term cycling at a C/2 rate between 1.8 and 2.7 V. Long-term cycling of the batteries was carried out using a MACCOR (4000 series) battery cycler and Neware battery cycler. For shuttle current measurements, we cycled the cells for 3 cycles and stopped them at the desired voltage in the discharge step. To compare the shuttle currents, we used coin cells with 0 M (as the reference), 0.02 M and 0.2 M TU additive and measured the shuttle current at 4 different potentials. For example, for the cells stopped at 2.3 V, we applied a constant potential of 2.3 V and held the cell at this potential for 2 h and recorded the current response. The shuttle current measurements and cyclic

voltammetry (CV) tests were carried out using a potentiostat (Gamry reference 1000).

3. Results and discussion

3.1 Redox activity of thiourea

Fig. 1a shows the SEM image of CNFs used as the cathode material in these cells. The fabrication method has been described in the Experimental section. The freestanding nature of the CNFs does not require the use of any binders or current collectors. To incorporate sulfur, we used the “ultra-rapid melt diffusion” technique developed in our lab.²⁵ In this technique, a desired amount of sulfur is sprinkled on CNFs and incorporated into the nanofiber mat using a hot press in only 55 s. The SEM images of SCNF cathodes used in this study are presented in Fig. 1b. The cross-sectional SEM images and elemental

mapping of SCNF cathodes are shown in the ESI, Fig. S1.† The elemental mapping in this figure confirms that sulfur is incorporated throughout the CNF mat thickness. To confirm the sulfur weight percent, the TGA curve of the SCNF cathode is presented and compared to the TGA plot of pure sulfur in Fig. 1c. The TGA results show that the sulfur weight% in the SCNF cathode is ~48%. A slight shift is observed in the decomposition temperature of sulfur in the SCNF cathode compared to pure sulfur powder. A similar trend was reported by our group in previous studies, where sulfur or sulfur-rich copolymers were used as the active material and incorporated into CNFs using a hot press.^{5,25} We believe that the slight shift observed is related to the enhanced heat transfer as a result of the increased surface area, which results in a lower decomposition temperature. The CNFs and SCNFs were dried under

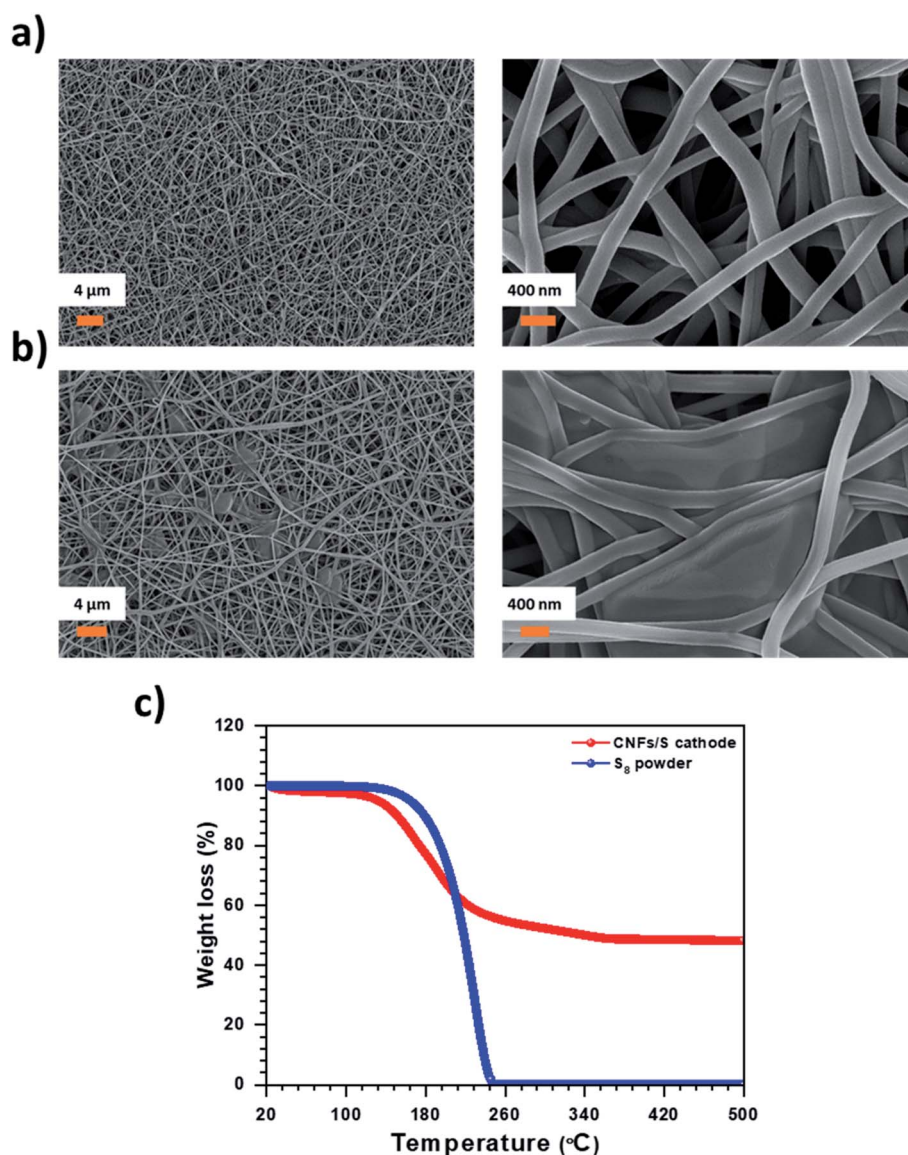


Fig. 1 (a) SEM image of CNFs, (b) SEM image of SCNFs, where sulfur is incorporated using the ultra-rapid melt diffusion technique, and (c) TGA result of sulfur powder and SCNF cathodes used in this study.

vacuum and used as the cathode without any further modification.

To understand the effect of the thiourea-based electrolyte additive on the performance of Li-S batteries, we first fabricated coin cells using CNFs as the cathode (without any sulfur active material). These coin cells are referred to as “blank cells” in the manuscript and serve as reference cells to understand thiourea activity without the interference of sulfur active material and eventually elucidate its interaction with polysulfides when sulfur is added. Fig. 2a shows the cyclic voltammetry (CV) curves of the blank cells with and without the thiourea additive. The black line represents a blank cell with a conventional ether-based electrolyte without thiourea. The other CVs in Fig. 2a are for similar coin cells at a scan rate of 0.02 mV s^{-1} , when 0.02 M TU is added to the electrolyte. As can be seen in this figure, two pairs of redox peaks, denoted as A/A' and B/B', appear when TU is added to the electrolyte. The reduction peaks at ~ 2.4 (denoted as A) and $\sim 2.0 \text{ V}$ (denoted as B) and oxidation peaks at $\sim 2.2 \text{ V}$ (denoted as B') and $\sim 2.4 \text{ V}$ (denoted as A') confirm that TU has a redox activity in the ether-based electrolyte. Note that the peaks are consistently present over five cycles, with almost the same intensity, confirming the reversible nature of the redox behavior of TU. Although, TU is known to have redox activity in aqueous acidic or alkaline media,^{26–30} however, to date there is no report focusing on the reversible

redox activity of the TU additive in a non-aqueous environment. Fig. 2b shows the effect of the scan rate on the CV result of coin cells with the TU additive. The two redox peaks are still present at a high scan rate of 0.5 mV s^{-1} . Further increase in the scan rate results in the vanishing of the second cathodic peak (see Fig. S2a†). At higher scan rates, the anodic peak at $\sim 2.2 \text{ V}$ shifts to $\sim 2.35 \text{ V}$ and its intensity becomes very low. Following these experiments, we also carried out a cyclic voltammetry experiment over an extended potential range, from 1.4 V to 3 V at 0.1 mV s^{-1} . The result of this experiment is presented in Fig. S2b.† Bercot *et al.* reported that TU has an irreversible redox reaction in acetonitrile solvent.²⁷ Based on our results, there are two reversible redox pairs, and no irreversible reduction or oxidation peak was observed.

To understand the effect of TU concentration, we fabricated blank coin cells using 0.02 M , 0.2 M and 0.5 M thiourea additives. Fig. 2c shows the CV results of these coin cells. It is clear from this figure that the intensity of the redox peaks becomes stronger as the thiourea concentration increases, corroborating that the peaks are indeed associated with TU redox activity. To have a better understanding of the effect of the TU additive, we have adjusted the y axis (current) in Fig. 2a and c based on the amount of TU used in the battery, see Fig. S2c and d.† As can be seen in Fig. S2d,† when current is adjusted based on the weight of TU used in the cell, a very similar current response is

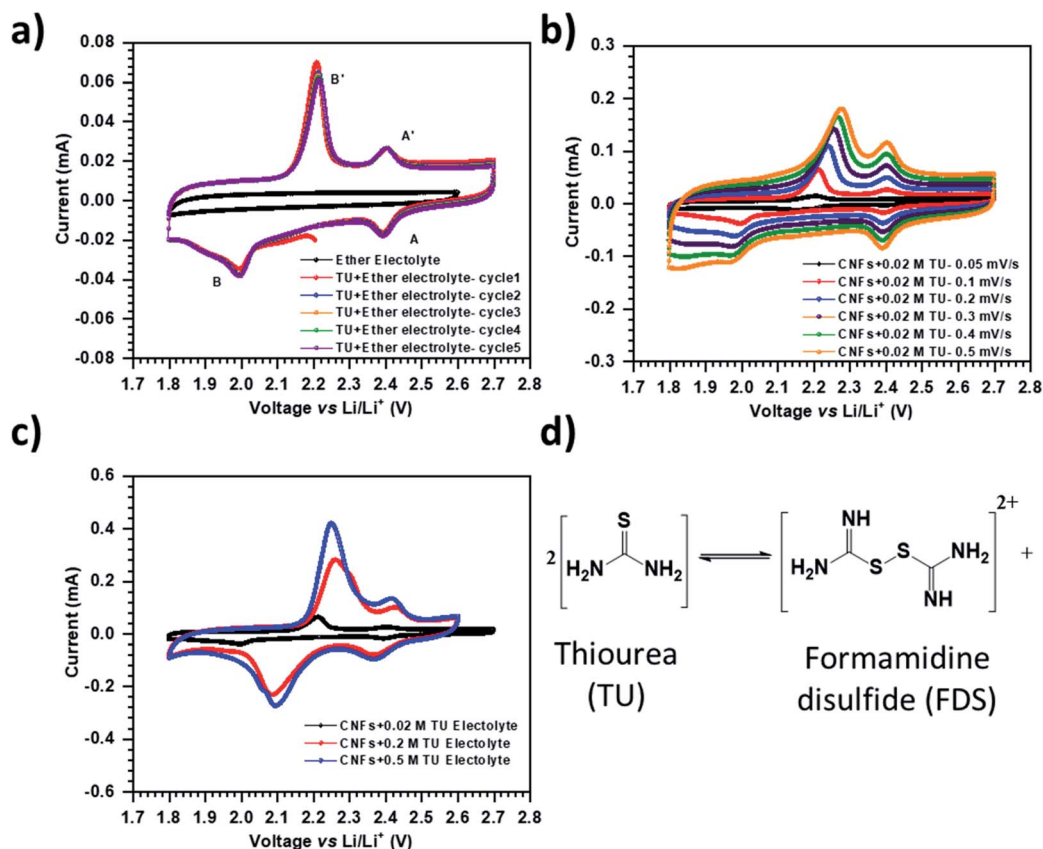


Fig. 2 Cyclic voltammetry results of (a) blank cells – CNFs (without S), with and without the TU additive at 0.02 mV s^{-1} , (b) CNFs with the 0.02 M TU additive added to the electrolyte at different scan rates, (c) CNFs when different concentrations of TU (0.02 , 0.2 , and 0.5 M) were added to the ether-based electrolyte, and (d) proposed electrochemical pathway for the redox activity of TU in an ether-based electrolyte.

measured. We believe that as a result of electrochemical reactions occurring at the electrode–electrolyte interface, thiourea reversibly converts to formamidine disulfide. The structure of thiourea and formamidine disulfide (FDS) and a hypothesized reaction pathway are presented in Fig. 2d. To confirm this hypothesis, we fabricated a slurry using commercial formamidine disulfide as the active material. The slurry was composed of formamide disulfide, PVDF and conductive carbon. The FDS cathode was used without further modification with ether-based electrolyte (without the TU additive). Fig. S3a† shows the CV results for FDS in the ether-based electrolyte. As shown in this figure, two redox peaks in cathodic and anodic scans are present. The reduction peaks at ~ 2.39 V and ~ 2.1 V are very similar to the peaks shown in Fig. 2a in the presence of TU. Moreover, the oxidation peaks at ~ 2.3 V and ~ 2.4 V are in a similar position to the TU redox peaks; however, the intensity of the peaks seems to be different. Based on the similarities in the CV results of TU and FDS, we hypothesize that the TU additive reversibly converts to FDS. We also carried out FTIR experiments of the electrolytes with TU after exposure to Li metal. Based on the results presented in Fig. S4,† thiourea molecules are not lithiated after exposure to Li metal. We believe that the redox behavior of TU is originated from the sulfur atom being oxidized and thus, a dimer is formed. The reduced sulfur atom forms a bond with another reduced sulfur atom, forming a disulfide bond (Fig. 2d). The disulfide is then reduced to its original state during the discharge. TU exists as a hybrid of different resonance mesomers, as presented in Fig. S3b.†³¹ The contribution of different mesomers is known to be affected by pressure, temperature or solvents.³² As a result of this resonance, the negative charge of the sulfur atom in its reduced state is not localized, so the electrochemical reaction is accelerated. This phenomenon can explain the electrochemical reaction of thiourea at high scan rates up to 10 mV s^{-1} . Similar electrochemical pathways have been reported in the literature for thiourea-based materials. Hiroshi *et al.* reported the electrochemical activity of the sulfur atom in thiourea or/and polymers with thiourea as its main polymeric unit.³¹ This study investigated thiourea-based compounds as electrode materials for lithium secondary batteries using a gel polymer electrolyte. Based on this report, the sulfur atom in thiourea is responsible for the reversible electrochemical reactions by forming a disulfide bond with sulfur from another TU compound. The result of this study is in agreement with our hypothesis of the formation of the C–S bond when TU is used as an electrolyte additive in Li–S battery.

3.2 Effect of the thiourea additive on the performance of Li–S batteries

To demonstrate the effect of the TU additive on the performance of Li–S batteries, the freestanding SCNF cathodes, with a loading of 1.2 to 1.4 mg cm^{-2} , were used. To evaluate the effect of the thiourea additive, we fabricated cells using 0 M (*i.e.* ether electrolyte without TU, as a reference), 0.02 M , and 0.2 M TU. Fig. 3a shows the CV results for these batteries. As can be seen from the CV results, the reference electrolyte shows two typical reduction

peaks. The first one corresponds to the formation of long chain polysulfides (Li_2S_x , $6 \leq x \leq 8$) and the second one corresponds to the conversion of long chain polysulfides to short chain polysulfides (Li_2S_x , $x < 6$), and their final conversion to the Li_2S solid discharge product. The two reduction peaks appear at ~ 2.30 V and ~ 1.95 V in the reference cell (*i.e.*, an ether-based electrolyte without the TU additive). When the TU additive is added to the electrolyte, there is a clear shift toward higher voltage in each reduction peak of the Li–S battery. For the coin cell with 0.2 M TU (blue line in Fig. 3a), the first reduction peak appears at ~ 2.34 V and the second peak at ~ 2.02 V, corresponding to $\sim 400 \text{ mV}$ and $\sim 70 \text{ mV}$ shifts from those of the reference cell, respectively. Moreover, a small shoulder is seen in the second reduction peak, which might be originating from the redox activity of the TU additive. The broad oxidation peak, on the other hand, shifted toward a lower voltage, when the TU additive was used. Based on the CV results in Fig. 3a, the TU additive decreases the polarization of the cell, possibly by facilitating the deposition of Li_2S (in the discharge process) and utilization of Li_2S (in the charging process) of the battery. These results are interesting because the addition of TU to the electrolyte is expected to decrease the ionic conductivity of the electrolyte, which in fact can have the opposite effect of increased cell polarization. Ho *et al.*, for example, showed that the ionic conductivity, at room temperature, of an ether-based electrolyte was decreased from $\sim 1.2 \times 10^{-5} \text{ S cm}^{-1}$ to $\sim 1.0 \times 10^{-5} \text{ S cm}^{-1}$ in the presence of the 1.0 M TU additive.²³ The decrease in the polarization of the battery, despite the increase in electrolyte resistance, confirms that the TU additive can facilitate the kinetics of the redox reaction in Li–S batteries. We believe that TU can act as a redox mediator (discussed later) to enhance the kinetics of Li–S batteries.

The long-term cycling result of batteries with and without the TU additive is presented in Fig. 3b. All cells were conditioned at C/10 and C/5 rates for two cycles each, before long-term cycling at C/2 (where $1\text{C} = 1675 \text{ mA h g}^{-1}$). As can be seen in this figure, the capacity of the reference Li–S battery (with an ether-based electrolyte without the TU additive) continuously decreases within 300 cycles. On the other hand, cells with only 0.02 M TU additive show relatively stable cycling up to 300 cycles with a capacity of $\sim 525 \text{ mA h g}^{-1}$ after 300 cycles. Further increase in the TU concentration results in a very stable cycling with higher capacity compared to the previous cells. The coin cell with the 0.2 M TU additive, showed a capacity of $\sim 780 \text{ mA h g}^{-1}$ after 300 cycles. The long-term cycling of the coin cell with 0.2 M TU up to 700 cycles is presented in Fig. 3c. The capacity of this cell was stabilized to 839 mA h g^{-1} after 5 cycles with a capacity decay rate of 0.025% per cycle and with a coulombic efficiency of more than 97% throughout the cycling. Moreover, as mentioned earlier, TU is a redox active material in the potential window of Li–S batteries. To understand the contribution of this additive to the capacity of the batteries, we have calculated the theoretical capacity of TU based on 1e^- transfer per mole of TU, and adjusted this number based on the weight of active material used. Our calculations, presented in the ESI,† show that 0.02 M and 0.2 M TU added to the reference ether electrolyte can contribute up to

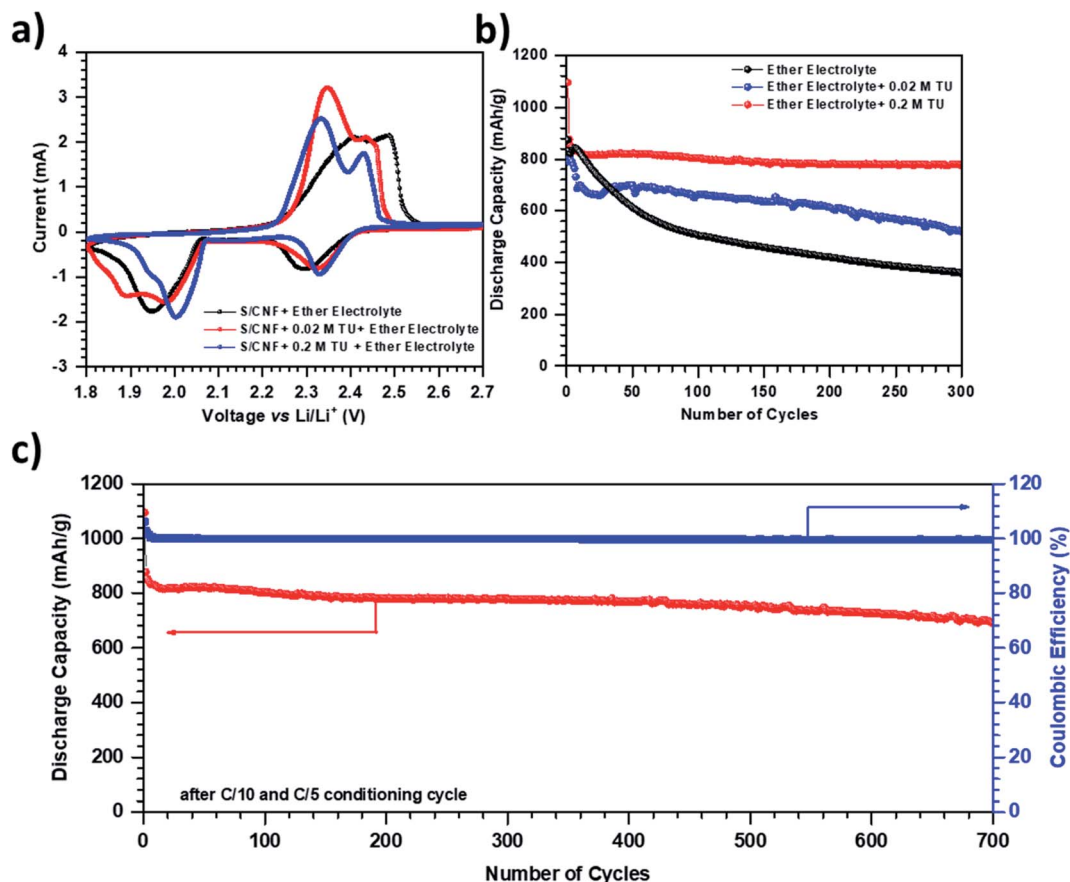


Fig. 3 (a) Cyclic voltammetry results of SCNf cathodes, with and without the TU additive at 0.02 mV s⁻¹, (b) cycling results of SCNfs in an ether-based electrolyte, compared to when 0.02 M TU and 0.2 M TU are added to the ether-based electrolyte, and (c) long-term cycling and coulombic efficiency results of 0.2 M TU in the ether electrolyte.

10.72 mA h g⁻¹ and 107.2 mA h g⁻¹ and 268 mA h g⁻¹, respectively.

Based on the electrochemical results discussed so far, we can conclude that the TU additive can have a tremendous effect on decreasing the cell polarization and enhancing the capacity and cycle life of Li-S batteries. We believe that these improved results can be attributed to the dual role of the TU additive in Li-S batteries. The first role is the positive effect of TU as a shuttle inhibitor. TU can be used to control and delay the polysulfide shuttle phenomena. Moreover, we hypothesize that this additive can act as a redox mediator to facilitate the kinetics of the reaction in each discharge and charge half cycle. To investigate our hypothesis, we designed a series of electrochemical experiments, as discussed below. To show the effect of TU on reducing the polysulfide shuttling, we measured the steady-state shuttle current of Li-S batteries with and without the TU additive. To confirm the role of TU as a redox mediator, we synthesized Li₂S decorated carbon nanofibers (Li₂S/CNFs) and used them as a cathode in a Li-S battery (without any additional sulfur). We then compared the Li₂S activation in the first charging step, with and without the TU additive.

3.3 Thiourea as a shuttle inhibitor additive

The long cycle life of a Li-S battery, along with the high coulombic efficiency throughout the cycling, is considered to be an indicator of shuttle control in Li-S batteries.^{1,33} Mikhaylik *et al.* attempted to quantify the redox shuttle in Li-S batteries using a combination of mathematical models and experimental results, introducing the “charge-shuttle factor”.³⁴ More recently, a new electrochemical approach, termed as “steady-state shuttle current” measurement, was introduced by Moy *et al.*³⁵ This simple but direct measurement of the shuttle current provides a better insight into the effect of using different additives or host materials to overcome the PS shuttle challenge.^{36–38} The overall idea behind this measurement relies on the decrease in the cell potential as a result of the polysulfide diffusion from the cathode to the anode. Hence, the shuttle current is basically the faradaic current needed to balance the polysulfide shuttle from the cathode to the anode. We fabricated coin cells with different concentrations of TU, starting from 0 M (reference cell) to 0.02 M and 0.2 M TU. The cells were cycled for three cycles at 0.1 mV s⁻¹ and stopped at various potentials. The cell potential was then kept constant at the corresponding potential and the current response was recorded using a potentiostat. This experiment was repeated at four different potentials. It is

important to note that to avoid any false results, we have used cathodes with a similar sulfur loading and wt%. This is because the polysulfide concentration at each given voltage strongly depends on the sulfur loading, and the measured shuttle current is a representation of the concentration gradient across the cell. Fig. 4 shows the effect of TU concentration on the shuttle current measured at 2.3 V for 2 hours. The shuttle current measurement at ~ 2.3 V corresponds to the formation of Li_2S_6 , which is known to be the most soluble polysulfide species in the ether-based electrolyte. As can be seen in Fig. 4, there is a transient region which arises from the small difference between the open circuit voltage of the cell and the potential at which the measurement is carried out. This transient region is followed by a steady state region, known as the shuttle current. The measured shuttle current drops from $\sim 0.6 \text{ mA cm}^{-2}$ to $\sim 0.1 \text{ mA cm}^{-2}$ in the presence of 0.02 M TU, which is almost a 6-fold drop in the shuttle current measured at 2.3 V. Moreover, by increasing the TU concentration to 0.2 M, the measured shuttle current further decreases to almost zero. Based on the discussion presented, the decrease in the shuttle current in the presence of the TU additive is a direct sign of reduced polysulfide shuttling. Moreover, as can be seen in Fig. 4, the shuttle current gradually decreases when no TU is used; however, when 0.2 M TU is added to the electrolyte, the shuttle current remains very stable for two hours. The gradual decrease in the measured current shows that the concentration gradient changes over time. This decrease can be attributed to the formation of insoluble products on the anode side.³⁵ Fig. S5a–c† present the shuttle current measurement at 2.1 V, 2.0 V, and 1.9 V. The negative sign of the shuttle current corresponds to the beginning of the formation of insoluble products. The appearance of the negative sign at 2.1 V only for 0.2 M TU confirms that the formation of insoluble products (at the second peak in CV results) occurs earlier when 0.2 M TU is used. These results further confirm the conclusions from CV results discussed before. We believe that there are three possible ways in which TU can bind lithium polysulfides and reduce their shuttling

during the cycling of Li–S batteries. The C=S and the amine functional group in the TU additive can bind lithium polysulfides formed during discharge. For example, a binding energy of $\sim 1.13 \text{ eV}$ is reported between nitrogen in the amine group and Li_2S via polar–polar interaction.³⁷ Moreover, as discussed before, the FDS formation as a result of electrochemical oxidation of the TU additive can also contribute to the binding of PSs. Once the S–S bond in FDS (C–S–S–C) breaks, the two radicals formed at the terminal sulfurs, connected to carbon, can bind the $\text{S}_3^{\cdot -}$ formed in the discharge process of Li–S batteries. A similar binding mechanism is reported previously using thiol-based additives for Li–S batteries.¹⁷

3.4 Thiourea as a redox mediator additive

Apart from this additive's positive role in inhibiting the PS shuttling, we believe that TU can also serve as a redox mediator to enhance the kinetics of reactions. RMs can accelerate the kinetics of the reaction and improve the performance of batteries by utilizing the active material in each charge and discharge half cycle.^{15,22,39} The use of redox mediators in Li–S batteries becomes vital as the Li_2S discharge product is ionically and electronically insulating.^{40–42} As a result, a large overpotential is needed to overcome the energy barrier of Li_2S . We believe that TU as a redox mediator can help re-utilize the Li_2S particles that are not in direct contact with the conductive host material, here CNFs. To investigate this hypothesis, we synthesized a $\text{Li}_2\text{S}/\text{CNFs}$ cathode material, using electrospinning. We adopted and modified a previous method report in the literature to fabricate Li_2S -based cathodes outside a glovebox.⁴³ PVP was used as the carbon source and Li_2SO_4 as a precursor to synthesize Li_2S using a thermal treatment ($\text{Li}_2\text{SO}_4 + 2\text{C} \rightarrow \text{Li}_2\text{S} + 2\text{CO}_2$). It is worth mentioning that by using electrospinning, the whole synthesis procedure was carried out outside a glovebox and the nanofibers were transferred inside right after the final heat treatment under argon flow. Fig. 5a and b show the SEM picture of $\text{Li}_2\text{S}/\text{CNFs}$ electrodes and their elemental mapping. As can be seen in this figure, the $\text{Li}_2\text{S}/\text{CNF}$ cathode material has a porous structure which can help in Li_2S utilization. The porous structure of this material might be a result of using acetone as a cosolvent in electrospinning. A similar result is reported by Megelski *et al.*, examining the properties of electrospun polyester fibers using various ratios of DMF (less volatile) and THF (more volatile).⁴⁴ Based on the result of their study, a vapor-induced phase separation is responsible for the pore formation. The formation of pores is determined by the vapor pressure (or boiling point) of the nonsolvent and polymer concentration. The sulfur elemental mapping confirms that Li_2S particles are uniformly distributed in the $\text{Li}_2\text{S}/\text{CNF}$ cathode material. Moreover, the formation of Li_2S decorated CNFs is confirmed using XRD. Fig. 5c shows the XRD results of the $\text{Li}_2\text{S}/\text{CNF}$ cathode. To carry out this experiment, we sealed $\text{Li}_2\text{S}/\text{CNFs}$ using Kapton tape inside a glovebox. The XRD of Kapton tape is also presented in Fig. 5c as a reference and it confirms that the crystalline peaks are solely from the presence of Li_2S particles. As can be seen in Fig. 5c, the 2θ peaks at $\sim 26, 32, 45, 53$, and 58 degrees confirm the formation

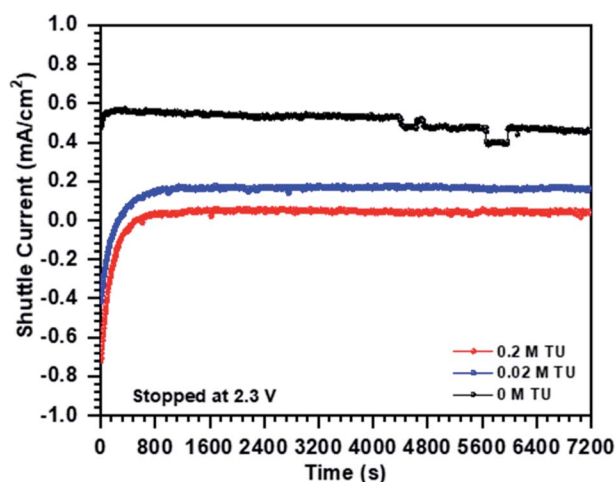


Fig. 4 Steady-state shuttle current measurement at 2.3 V with and without TU electrolyte additive.

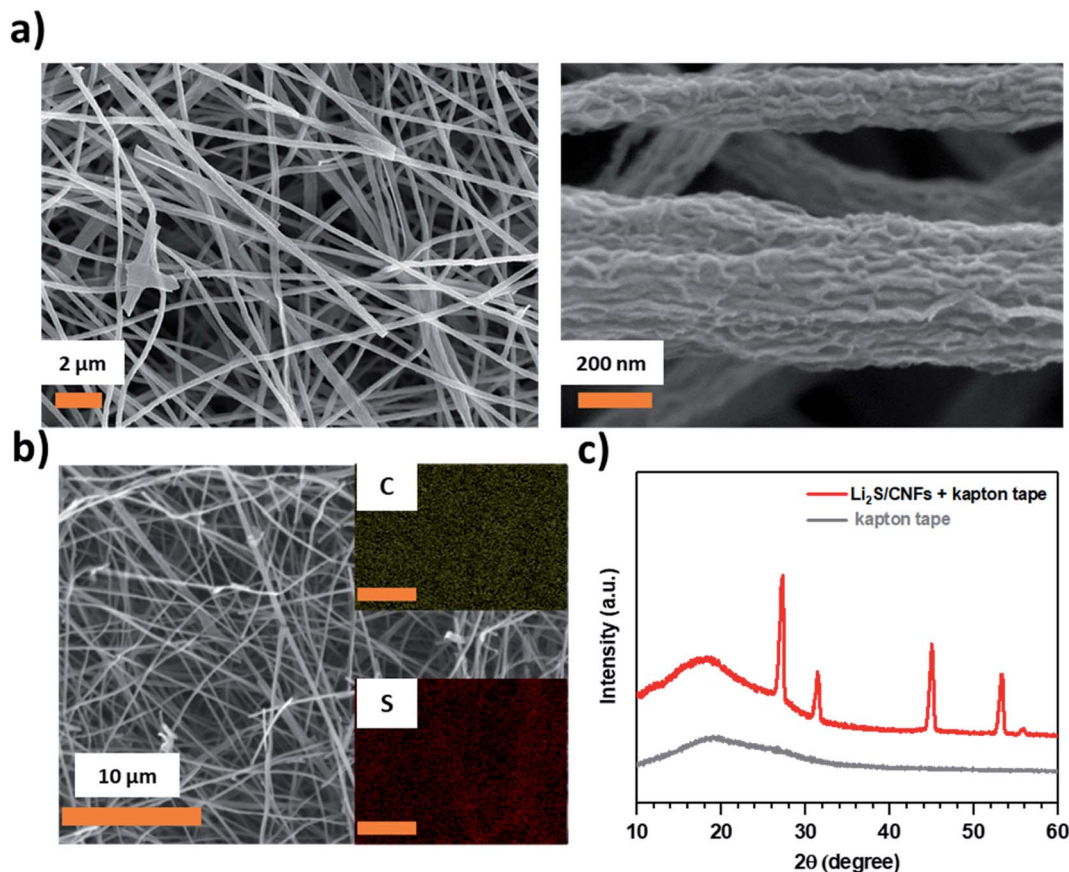


Fig. 5 (a) SEM image of the $\text{Li}_2\text{S}/\text{CNF}$ cathode fabricated using the electrospinning technique, (b) SEM image and elemental mapping of the $\text{Li}_2\text{S}/\text{CNF}$ cathode, and (c) XRD result of $\text{Li}_2\text{S}/\text{CNF}$ sealed with Kapton tape and XRD of Kapton tape for reference.

of Li_2S decorated CNFs. To confirm that the TU additive can be used as a RM to facilitate Li_2S utilization, we fabricated coin cells using $\text{Li}_2\text{S}/\text{CNFs}$ as the cathode, and we compared the electrochemical results with and without the addition of the TU additive. The $\text{Li}_2\text{S}/\text{CNF}$ based coin cells were charged to 3.8 V at a C/20 rate ($1\text{C} = 1166 \text{ mA h g}_{\text{Li}_2\text{S}}^{-1}$), to compare the utilization of Li_2S and its conversion to S_8 . It is worth mentioning that the redox activity of TU is at a slightly higher voltage than the theoretical potential for Li_2S oxidation (~ 2.15), which makes it an ideal candidate for a redox mediator.¹⁵ Fig. 6a shows the galvanostatic charging for the first charging half-cycle of the batteries using Li_2S as the cathode material. As can be seen from this figure, the activation overpotential for a conventional Li_2S -based cathode is not observed in our results. The mitigation of such overpotential might originate from the nanofibrous morphology and enhanced surface area of $\text{Li}_2\text{S}/\text{CNFs}$. Nevertheless, there are clear differences between the voltage plateaus in the presence of the TU additive. The cell without an additive shows a small potential plateau at ~ 2.9 V followed by a larger plateau at ~ 3.5 V, with most of the capacity or Li_2S activation originating from the second plateau. However, by adding 0.2 M TU, the plateau contributing to Li_2S activation shifts to ~ 2.5 V. In other words, if the cut-off voltage of cells with $\text{Li}_2\text{S}/\text{CNFs}$ was set to 3.0 V, the capacity of the cell with TU would be $\sim 679 \text{ mA h g}^{-1}$, whereas the reference cell without the TU

additive would only deliver a capacity of $\sim 183 \text{ mA h g}^{-1}$. The battery with 0.2 M TU as an additive shows a capacity of 1080 mA h g^{-1} , which is clearly higher than that of the battery without the TU additive ($\sim 620 \text{ mA h g}^{-1}$) in the first charging step. Fig. 6b shows the charge–discharge curves of the $\text{Li}_2\text{S}/\text{CNF}$ cathode after the activation step (first discharge), which shows the two-potential plateau behavior of the $\text{Li}_2\text{S}/\text{CNF}$ cathode with and without the TU additive in Li–S batteries. However, similar to the charging step, the first discharge capacity of $\text{Li}_2\text{S}/\text{CNF}$ cathodes was enhanced from 588 mA h g^{-1} to 1005 mA h g^{-1} by adding 0.2 M TU to the reference ether electrolyte. The role of TU in facilitating this conversion is not limited to the first cycle only. Based on these electrochemical results, we believe that TU acts as a redox mediator to facilitate the conversion of Li_2S to S . Scheme 1 shows the proposed dual role of TU as an additive to reduce the shuttling of PSs and as a redox mediator in the discharge and charge step of Li–S batteries.

3.5 Broad applicability of TU in the development of practical cells

In this final section, we demonstrate the broad applicability and benefit of thiourea in cells with more practical cathode designs. In the first example, we built a lithium metal-free cell with a commercial graphite anode, Li_2S -based cathode and 0.2 M TU

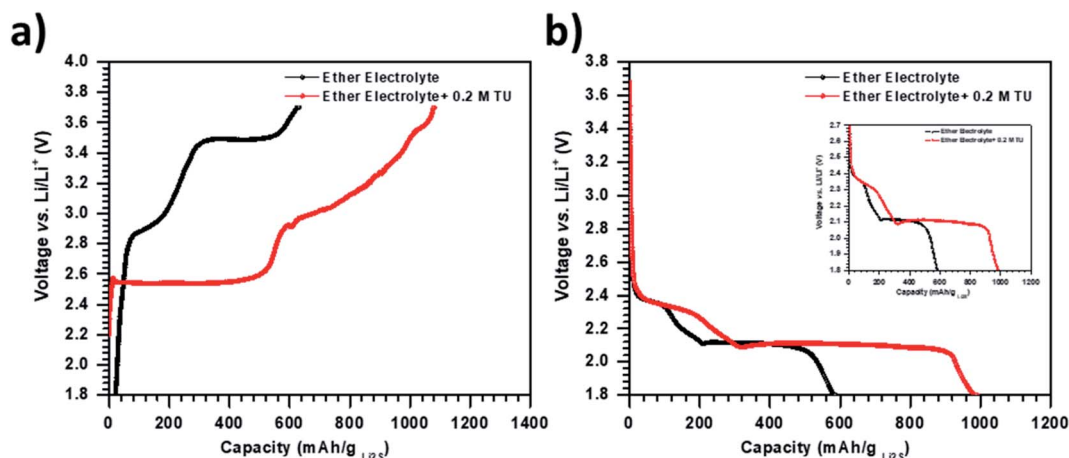
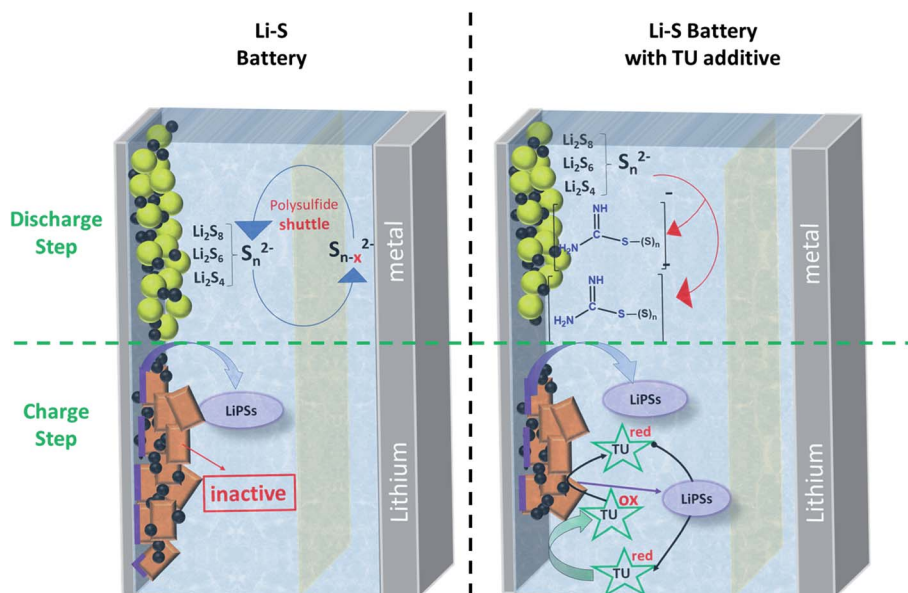


Fig. 6 (a) Galvanostatic charge–discharge plot for the first charge half cycle of the $\text{Li}_2\text{S}/\text{CNF}$ cathode at C/20, and (b) charge–discharge curves of the subsequent discharge step of the $\text{Li}_2\text{S}/\text{CNF}$ cathode at C/20; inset shows a zoomed-in view between 1.8 and 2.7 V.



Scheme 1 The role of TU as electrolyte additive in reducing polysulfide shuttling in the discharge step and redox mediation in the charge step.

in a standard ether electrolyte. This cell retains a capacity of $\sim 1007 \text{ mA h g}^{-1}$ at a C/2 rate after 400 cycles, 4 to 5-fold higher than that of typical Li-ion battery cathodes. The cycling result of this cell is presented in Fig. S6† and shows the potential of the TU additive in enabling the combination of the Li_2S cathode with a negative anode material in a dry room without the need for anode lithiation.⁴⁰ Such a battery could address all safety concerns around the use of a pure lithium anode, while still providing a capacity several fold higher than that of Li-ion batteries.

In the second example, we built lithium–sulfur cells using a lithium metal anode and a simple slurry-based cathode fabricated *via* just blending commercial sulfur with carbon black and PVDF binder. Although, slurry-based cathodes have

the disadvantage of added weight because of the insulating binder and current collector, they are commonly used in industry. Moreover, numerous research papers have demonstrated rapid capacity fade in such cathodes in ether electrolytes due to shuttling and will therefore serve as a great candidate to demonstrate the practical advantage of the thiourea additive and its applicability to various types of sulfur cathodes. Our Li–S batteries fabricated using these cathodes with a loading of $1.4\text{--}1.6 \text{ mg cm}^{-2}$ showed a stable capacity of $\sim 575 \text{ mA h g}^{-1}$ at a C/2 rate even after 700 cycles when TU was added, whereas the reference battery without TU reaches $\sim 150 \text{ mA h g}^{-1}$ (Fig. 7a). The initial capacity drop observed in Fig. 7a is a common observation in the Li–S battery field. Although the exact reason behind this initial capacity drop is unclear, it can be attributed

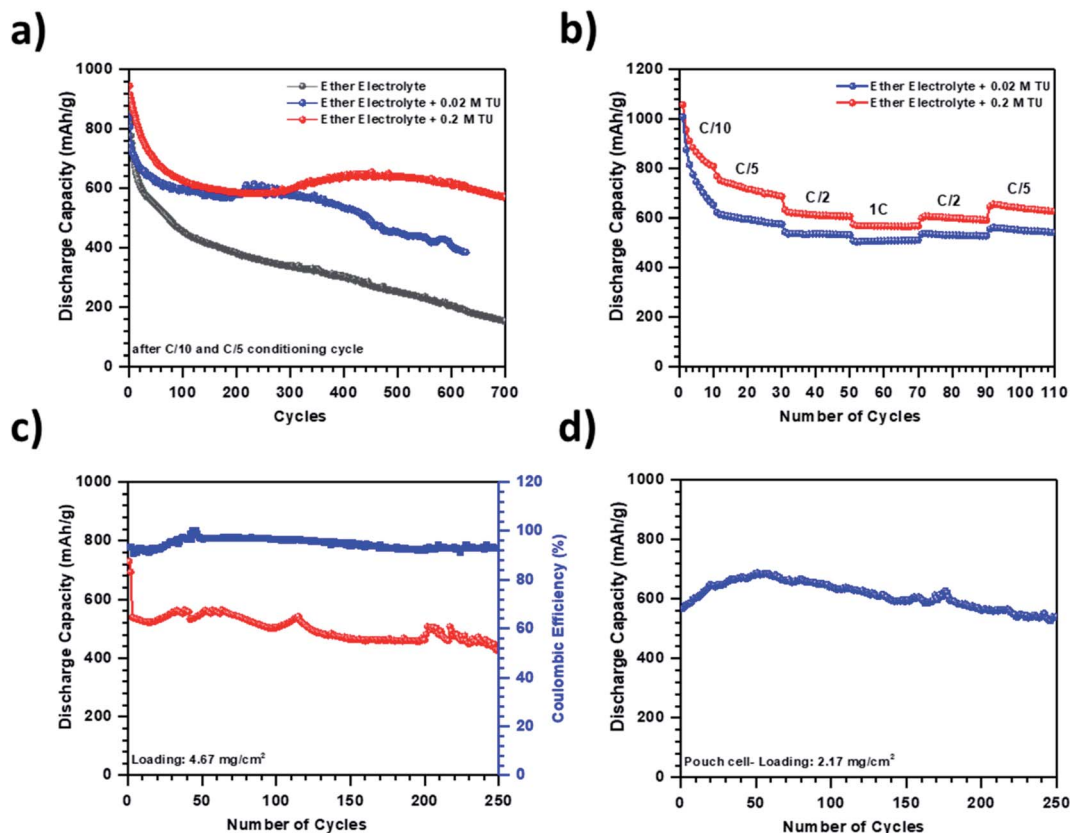


Fig. 7 (a) A comparison between the long term cycling results of sulfur slurry cathodes in ether-based electrolytes with and without the TU additive at C/2 rate, (b) rate-capability test results of Li-S batteries using slurry cathodes in presence of TU electrolyte additive at different C-rates, (c) cycling results for a slurry cathode with a high loading of $\sim 4.7 \text{ mg cm}^{-2}$, with 0.2 M TU added to the ether-based electrolyte at C/5 rate, and (d) cycling result of a pouch cell Li-S battery with 0.2 M TU at C/5 rate.

to the required time/cycles for polysulfides to reach equilibrium in the cell.^{45,46} In addition, Thieme *et al.* correlated the initial drop to the E/S ratio and suggested that an optimum polysulfide concentration might help in avoiding the irreversible loss and consequently the initial drop.⁴⁷ Moreover, we increased the sulfur loading of the cell to 2–2.1 mg cm^{-2} (see Fig. S7†) and achieved stable cycling up to 300 cycles. We determined the rate capability of these cells by testing at rates all the way up to 1C. The cells without TU do not operate at such high rates, because of slow kinetics and high polarization.³³ Fig. 7b shows the successful rate capability test results using the TU additive. Fig. 7c shows cells with a practical sulfur loading of 4.7 mg cm^{-2} . They exhibit a capacity of $\sim 730 \text{ mA h g}^{-1}$, which stabilizes to $\sim 525 \text{ mA h g}^{-1}$ after 10 cycles and remains stable up to 250 cycles, with its coulombic efficiency being $\sim 97\%$. It is important to note that in the literature, these slurry cathodes (carbon black/S/binder) typically fail in less than 100 cycles, even with low S loadings of $\sim 1 \text{ mg cm}^{-2}$.⁴⁸ High loading data are specifically important, because it is reported that a sulfur loading of $\sim 5\text{--}6 \text{ mg cm}^{-2}$ is required to achieve an energy density of $\sim 500 \text{ W h kg}^{-1}$, which seems to be a practically relevant result.^{19,33,49} Finally, we built prototype pouch cells with a 25 cm^2 electrode area using slurry cathodes and 0.2 M thiourea (Fig. 7d). The initial increase in the capacity is possibly due

to insufficient electrolyte wetting in the large area cells. The pouch cell retained a capacity of $\sim 601 \text{ mA g}^{-1}$ after 10 cycles and remained stable up to 250 cycles with a low capacity decay rate of 0.042% per cycle.

4. Conclusions

In this study, we have introduced thiourea as a redox active electrolyte for Li-S batteries. Using the TU additive, the SCNF cathode showed a capacity of $\sim 839 \text{ mA h g}^{-1}$ after 5 cycles. This capacity remained stable over 700 cycles with a low capacity decay of 0.025% per cycle and coulombic efficiency of $>97\%$. On the other hand, the capacity of the reference battery without the TU additive continuously dropped over 300 cycles. We demonstrated that the outstanding performance of batteries with TU electrolyte additive originates from the dual role of this additive as a redox mediator and shuttle inhibitor. To show the polysulfide suppression role of this additive, we used the steady-state shuttle current measurements at four different discharge states. The shuttle current measured showed a 6-fold decrease in the steady state shuttle current when only 0.02 M TU was added to the ether-based electrolyte. Moreover, to show the redox mediation role of TU, we fabricated cells using a Li_2S cathode and showed a significant decrease in the activation

potential of Li_2S cathodes in the presence of TU. To further illustrate the broad application of these additives we have studied two more systems. The first system is a Li metal-free cell, with graphite as the anode and Li_2S as the cathode material. This cell shows a stable capacity of $\sim 1007 \text{ mA h g}^{-1}$ after 400 cycles. The second system relies on using a simple industry-friendly carbon/sulfur slurry in coin cell and pouch cell Li-S batteries. Our results show stable cycling of Li-S batteries with a 25 cm^2 carbon/sulfur slurry cathode over 250 cycles with a capacity decay rate of 0.042% per cycle. As indicated in this study, on addition of only 0.2 M TU, a significant improvement in practical Li-S batteries is achieved. To demonstrate the significant role of the thiourea additive in improving the performance of Li-S batteries, we summarized the recent literature on electrolyte additives. As can be seen in Table S1,† owing to the dual role of thiourea, the addition of only 0.2 M of this additive to ether electrolytes results in stable cycling for 700 cycles, whereas other electrolyte additives improve the cycle life of Li-S batteries for a maximum of 500 cycles. Based on the results presented, this study provides a good starting point for further research in designing electrolyte additives with multiple roles.

Funding sources

This work was funded by the National Science Foundation (NSF-1804374 and NSF-1919177).

Author contributions

The manuscript was written through the contributions of all authors. All authors have approved the final version of the manuscript.

Conflicts of interest

The authors declare no competing financial interests.

Acknowledgements

The authors would like to thank Dr Jinwon Kim and Dr Arvinder Singh for the insightful discussions, the Materials Characterization Core at Drexel University for providing access to SEM and XRD. We thank Dr Palmese's group for providing TGA.

References

- 1 A. Manthiram, Y. Fu, S.-H. Chung, C. Zu and Y.-S. Su, *Chem. Rev.*, 2014, **114**, 11751–11787.
- 2 M. Wild, L. O'Neill, T. Zhang, R. Purkayastha, G. Minton, M. Marinescu and G. Offer, *Energy Environ. Sci.*, 2015, **8**, 3477–3494.
- 3 R. Demir-Cakan, *Li-S Batteries: The Challenges, Chemistry, Materials, and Future Perspectives*, World Scientific Publishing Europe, 2017.
- 4 L. Borchardt, M. Oschatz and S. Kaskel, *Chem.–Eur. J.*, 2016, **22**, 7324–7351.
- 5 A. Rafie, A. Singh and V. Kalra, *Electrochim. Acta*, 2021, **365**, 137088.
- 6 A. Singh and V. Kalra, *ACS Appl. Mater. Interfaces*, 2018, **10**, 37937–37947.
- 7 X. Liu, J. Q. Huang, Q. Zhang and L. Mai, *Adv. Mater.*, 2017, **29**, 1601759.
- 8 Q. Pang, X. Liang, C. Y. Kwok and L. F. Nazar, *Nat. Energy*, 2016, **1**, 1–11.
- 9 R. Fang, J. Xu and D.-W. Wang, *Energy Environ. Sci.*, 2020, **13**, 432–471.
- 10 R. Mukkablal and M. R. Buchmeiser, *J. Mater. Chem. A*, 2020, **8**, 5379–5394.
- 11 N. Akhtar, X. Sun, M. Y. Akram, F. Zaman, W. Wang, A. Wang, L. Chen, H. Zhang, Y. Guan and Y. Huang, *J. Energy Chem.*, 2021, **52**, 310–317.
- 12 W. Yang, W. Yang, A. Song, L. Gao, G. Sun and G. Shao, *J. Power Sources*, 2017, **348**, 175–182.
- 13 A. Singh, A. Rafie and V. Kalra, *Sustainable Energy Fuels*, 2019, **3**, 2788–2797.
- 14 N. Angulakshmi and A. M. Stephan, *Front. Energy Res.*, 2015, **3**, 17.
- 15 Y. Tsao, M. Lee, E. C. Miller, G. Gao, J. Park, S. Chen, T. Katsumata, H. Tran, L.-W. Wang and M. F. Toney, *Joule*, 2019, **3**, 872–884.
- 16 L. Zhang, M. Ling, J. Feng, L. Mai, G. Liu and J. Guo, *Energy Storage Mater.*, 2018, **11**, 24–29.
- 17 H.-L. Wu, M. Shin, Y.-M. Liu, K. A. See and A. A. Gewirth, *Nano Energy*, 2017, **32**, 50–58.
- 18 F. Wu, J. T. Lee, N. Nitta, H. Kim, O. Borodin and G. Yushin, *Adv. Mater.*, 2015, **27**, 101–108.
- 19 J. Robinson, K. Xi, R. V. Kumar, A. C. Ferrari, H. Au, M.-M. Titirici, A. P. Puerto, A. Kucernak, S. D. Fitch and N. Garcia-Araez, *J. Phys.: Energy*, 2021, 031501.
- 20 Z. W. Zhang, H. J. Peng, M. Zhao and J. Q. Huang, *Adv. Funct. Mater.*, 2018, **28**, 1707536.
- 21 Y. Chen, S. A. Freunberger, Z. Peng, O. Fontaine and P. G. Bruce, *Nat. Chem.*, 2013, **5**, 489.
- 22 S. Meini, R. Elazari, A. Rosenman, A. Garsuch and D. Aurbach, *J. Phys. Chem. Lett.*, 2014, **5**, 915–918.
- 23 V.-C. Ho, D. T. Ngo, H. T. Le, R. Verma, H.-S. Kim, C.-N. Park and C.-J. Park, *Electrochim. Acta*, 2018, **279**, 213–223.
- 24 C. Tran and V. Kalra, *J. Power Sources*, 2013, **235**, 289–296.
- 25 C. Dillard, S.-H. Chung, A. Singh, A. Manthiram and V. Kalra, *Mater. Today Energy*, 2018, **9**, 336–344.
- 26 A. E. Bolzán and L. M. Gassa, *J. Appl. Electrochem.*, 2014, **44**, 279–292.
- 27 M. Mouanga and P. Bercot, *Int. J. Electrochem. Sci.*, 2011, **6**, 1007–1013.
- 28 M. B. Q. Argañaraz, C. I. Vázquez and G. I. Lacconi, *J. Electroanal. Chem.*, 2010, **639**, 95–101.
- 29 A. Bolzan, T. Iwasita and A. Arvia, *J. Electroanal. Chem.*, 2003, **554**, 49–60.
- 30 J. Kirchnerová and W. C. Purdy, *Anal. Chim. Acta*, 1981, **123**, 83–95.
- 31 H. Uemachi, T. Sotomura, K. Takeyama and N. Koshida, *US5413883A*, 1995.

- 32 H. Tomkowiak and A. Katrusiak, *J. Phys. Chem. C*, 2018, **122**, 5064–5070.
- 33 A. Bhargav, J. He, A. Gupta and A. Manthiram, *Joule*, 2020, **4**, 285–291.
- 34 Y. V. Mikhaylik and J. R. Akridge, *J. Electrochem. Soc.*, 2004, **151**, A1969.
- 35 D. Moy, A. Manivannan and S. Narayanan, *J. Electrochem. Soc.*, 2014, **162**, A1.
- 36 C. Hu, H. Chen, Y. Shen, D. Lu, Y. Zhao, A.-H. Lu, X. Wu, W. Lu and L. Chen, *Nat. Commun.*, 2017, **8**, 1–9.
- 37 M. Xia, N. Zhang and C. Ge, *J. Mater. Sci.*, 2020, 1–9.
- 38 Z. Wang, Y. Dong, H. Li, Z. Zhao, H. B. Wu, C. Hao, S. Liu, J. Qiu and X. W. D. Lou, *Nat. Commun.*, 2014, **5**, 1–8.
- 39 X. Wu, N. Liu, B. Guan, Y. Qiu, M. Wang, J. Cheng, D. Tian, L. Fan, N. Zhang and K. Sun, *Adv. Sci.*, 2019, **6**, 1900958.
- 40 S. Li, D. Leng, W. Li, L. Qie, Z. Dong, Z. Cheng and Z. Fan, *Energy Storage Mater.*, 2020, **27**, 279–296.
- 41 Y. Liu, Y. Pan, J. Ban, T. Li, X. Jiao, X. Hong, K. Xie, J. Song, A. Matic and S. Xiong, *Energy Storage Mater.*, 2020, **25**, 131–136.
- 42 Y. Song, W. Cai, L. Kong, J. Cai, Q. Zhang and J. Sun, *Adv. Energy Mater.*, 2020, **10**, 1901075.
- 43 M. Yu, Z. Wang, Y. Wang, Y. Dong and J. Qiu, *Adv. Energy Mater.*, 2017, **7**, 1700018.
- 44 S. Megelski, J. S. Stephens, D. B. Chase and J. F. Rabolt, *Macromolecules*, 2002, **35**, 8456–8466.
- 45 G. Xu, J. Yuan, X. Tao, B. Ding, H. Dou, X. Yan, Y. Xiao and X. Zhang, *Nano Res.*, 2015, **8**, 3066–3074.
- 46 L. Yang, G. Li, X. Jiang, T. Zhang, H. Lin and J. Y. Lee, *J. Mater. Chem. A*, 2017, **5**, 12506–12512.
- 47 S. Thieme, J. Brückner, A. Meier, I. Bauer, K. Gruber, J. Kaspar, A. Helmer, H. Althues, M. Schmuck and S. Kaskel, *J. Mater. Chem. A*, 2015, **3**, 3808–3820.
- 48 M.-K. Song, Y. Zhang and E. J. Cairns, *Nano Lett.*, 2013, **13**, 5891–5899.
- 49 J. Liao and Z. Ye, *Batteries*, 2018, **4**, 22.